Dynamics of electric transport in interacting Weyl semimetals

B. Rosenstein[1,2] and M. Lewkowicz[2,*]

[1]*Electrophysics Department, National Chiao Tung University, Hsinchu 30050, Taiwan, Republic of China*

[2]*Physics Department, Ariel University, Ariel 40700, Israel*

(Received 25 April 2013; published 3 July 2013)

The response to an electric field (dc and ac) of electronic systems in which the Fermi "surface" consists of a number of three-dimensional (3D) Weyl points (such as some pyrochlore iridates) exhibits a peculiar combination of characteristics usually associated with insulating and conducting behavior. Generically a neutral plasma in clean materials can be described by a tight-binding model with a strong spin-orbit interaction. A system of that type has a vanishing dc conductivity; however the current response to the dc field is very slow: The current decays with time in a powerwise manner, different from an insulator. The ac conductivity, in addition to a finite real part $\sigma'(\Omega)$ which is linear in frequency, exhibits an imaginary part $\sigma''(\Omega)$ that increases logarithmically as a function of the UV cutoff (atomic scale). This leads to a substantial dielectric response like a large dielectric constant at low frequencies. This is in contrast to a two-dimensional (2D) Weyl semimetal-like graphene at a neutrality point where the ac conductivity is purely pseudodissipative. The Coulomb interaction between electrons is long range and sufficiently strong to make a significant impact on transport. The interaction contribution to the ac conductivity is calculated within the tight-binding model. The result for the real part expressed via the renormalized (at frequency $\overline{\Omega}$) Fermi velocity v is $\Delta\sigma'(\Omega) = e^4\Omega/(9\pi^2\hbar v)[2\log(\Omega/\overline{\Omega}) - 5]$.

DOI: 10.1103/PhysRevB.88.045108 PACS number(s): 72.80.Vp, 11.30.Rd, 11.15.Ha

I. INTRODUCTION AND SUMMARY

A long time ago a rather unorthodox physics of crystals possessing three-dimensional (3D) pseudorelativistic quasiparticles,[1] exhibiting an electronic dispersion relation $\varepsilon_{\mathbf{k}} = v|\mathbf{k}|$, where the velocity v is of the order of the Fermi velocity in regular condensed matter systems, was invoked to describe properties of Bi. The ultrarelativistic linear dispersion relation describes two conical bands (of opposite orientation) sharing the same cone tip. Recently several proposals[2–6] revived an interest in materials with such excitations nowadays called Weyl semimetals. The Fermi "surface" of such materials, typically with dominant spin-orbit interactions, consists just of a finite number of disconnected points (called Weyl or Dirac points, defined below) rather than forming a continuous Fermi surface like electrons in usual metals. The revived interest emerged of course after years of intense experimental and theoretical study of graphene, a 2D Weyl quasiparticle material.[7] Suspended graphene is just such a "semimetal" system and exhibits a number of remarkable properties. For example, despite having zero density of states at the Fermi level and ideally no impurities, it still has a nonzero dc conductivity.[8]

While this band "touching" at a singular point was noticed in band structure calculations even before the seminal work of Wallace on graphite,[9] the use of the Dirac model in 3D was in the context of the two-band approximation model of bismuth.[1] Due to the strong spin-orbit interaction, the linear in $\mathbf{k}$ terms in a low energy effective theory near the crystallographic point L of the fcc Brillouin zone, dominate over quadratic terms (that dominate near the Γ point, leading to a common "effective mass" description). The electronic excitations are described by an analog of the Weyl equation of particle physics, which describes eight two-component chiral spinors ψ (two for each of the four L points):

$$\partial_t \psi_\pm = \pm v\boldsymbol{\sigma}\cdot\boldsymbol{\nabla}\psi_\pm. \tag{1}$$

The sign describes the chirality of the mode. Metallic bismuth is only approximately described by the ultrarelativistic "massless" dispersion relation since the quasiparticles of the opposite chirality are coupled and form four-component massive Dirac bispinors. In Bi therefore electrons are not Weyl, but 10 meV massive Dirac electrons where, in addition, the Fermi level is located away from the Dirac point.

A number of related suggestions for suitable realizations of Weyl semimetals were recently put forward. Kariyado and Ogata[3] calculated the band structure of cubic inverse perovskites like Ca_3PbO with significant spin-orbit coupling. They observed the appearance of six Weyl points with a very small relativistic electron mass down to 4 meV on the line connecting the Γ and the X points. In iridium-based pyrochlores such as $Y_2Ir_2O_7$, there are $N_W = 24$ Weyl points located near the four L points of the fcc lattice. As noted in Ref. 2, these materials "in particular provide a unique opportunity to study the interplay of Coulomb interactions, spin-orbit coupling, and the band topology of solids." Also, strong spin-orbit interactions can lead to a phase of matter, the topological insulator[5] and various possibilities to create Weyl fermions combined into coincident opposite chirality points or separated in the Brillouin zone in BiO_2/SiO_2,[4] Na_3Bi, and $Hg_1Cr_2Se_4$.[6] These proposals generated a great deal of experimental efforts.[10] The system with 3D Weyl points was proposed to appear in optical lattices[11] following the discovery of "artificial graphene."[12]

Since the density of carriers in 3D Weyl semimetals at zero temperature is zero (as in suspended graphene in 2D), the Coulomb interactions are unscreened and therefore are expected to be important to the understanding of the electrical and optical response of these materials. Unsophisticatedly the dimensionless coupling

$$\alpha \equiv \frac{e^2}{\epsilon\hbar v} \tag{2}$$

is of order 1, provided the dielectric constant ϵ is not large, since the analog of the light velocity v is of the order typically of the Fermi velocity. Note that the same Coulomb potential $1/r$ created by an electron influences many more electrons in 3D compared to 2D, so naively, in 3D its importance is expected to increase. While electric transport in noninteracting 3D Weyl fermions was studied (Refs. 13 and 14 and references therein to earlier papers in the context of particle physics), the contributions of potentially very important Coulomb interactions (Coulomb scattering corrections to transport as an example) have not been studied theoretically, except basic renormalization effects.[14] This is in contrast to the situation in graphene.

The effect of the Coulomb interactions in undoped graphene turned out to be highly nontrivial, even within perturbation theory, and have evoked a scientific controversy[15–18] due to the problem of the "ultraviolet regularization," and was just recently settled[19] by noting that the ambiguities are associated with the treatment of the separation of scales related to the chiral anomaly.[20] Some aspects of the Weyl semimetal physics are *not* dominated by the Weyl points of the Brillouin zone at which the spectrum is gapless. For example, the ac conductivity of undoped graphene (the weak logarithmic renormalization of the electron velocity[21] does not influence the result) is given in terms of its value in the noninteracting theory $\sigma_0 = e^2/4\hbar$ by

$$\frac{\sigma(\Omega)}{\sigma_0} = 1 + C\alpha + O(\alpha^2) \tag{3}$$

and is strictly dissipative (real). This expression is independent of frequency (provided corrections of order $\hbar\Omega/\gamma$, $\gamma = 2.7$ eV being the hopping energy, are neglected). The value of the only numerical constant C appearing here has been a matter of intense controversy. The detailed calculation[15] utilizing a sharp momentum cutoff regularization of the Dirac model provided a value $C^{(1)} = \frac{25}{12} - \frac{\pi}{2} \approx 0.51$ of order 1. The use of the sharp momentum cutoff was criticized by Mishchenko,[16] who obtained an exceptionally small value of $C^{(2)} = \frac{19}{12} - \frac{\pi}{2} \approx 0.01$ making a "soft" momentum cutoff regularization. He supported this choice by the consistency of the Kubo and the kinetic equation calculations of conductivity with that of the polarization function. The consistency required a modification of the long-range interaction so that it becomes UV cutoff dependent. This apparently closed the issue. Albeit such a small numerical value would have profound physical consequences even beyond the transport and dielectric properties. Nevertheless, the interaction strength C was recalculated once again by Vafek *et al.*,[17] who argued that the modification of the interaction requires simultaneously a Pauli-Villars regularization of massless fermions. They applied yet another regularization, making the space dimensionality fractional, $D = 2 - \varepsilon$, that modified both the current operator and the interaction in such a way that they satisfy the Ward identities and obtained $C^{(3)} = \frac{11}{6} - \frac{\pi}{2} \approx 0.26$. The dimensional regularization is questionable on physical grounds and in a comprehensive subsequent work[18] the authors reaffirmed the small value $C^{(2)}$; it seems that this value is the commonly accepted one. The tight-binding calculation[19] however demonstrated that $C^{(3)}$ is the correct one. To reveal the origin of the ambiguity exhibited by the various values of C, the authors made use of a dynamical approach developed earlier[22] (to address the problem of separating the interband contributions from the intraband effects due to contacts[23,24]) directly in the dc case by "switching on" a uniform electric field in the tight-binding model with Coulomb interactions, and then considering the large-time limit. This approach (known in field theory as the "infinite hotel story") is the best way to reveal physical effects of anomalies.[25] One can directly separate the contributions from the neighborhood of Dirac points and the "anomalous" contributions from the rest of the Brillouin zone, so that one can decide what regularization of the effective Weyl theory is the correct one. In this sense this is advantageous over the standard diagrammatic Kubo formula calculation in continuum[15–18] that might encounter the so-called Schwinger terms (found in quantum electrodynamics, that is similar to the 3D Weyl fermions).

The purpose of the present paper is to study the effect of Coulomb interactions in 3D Weyl fermion systems with emphasis on dynamical aspects of electric transport and compare/contrast it with the corresponding results in 2D Weyl fermions. To achieve this goal we define in Sec. II a tight-binding description of Weyl fermions on a hypercubic lattice of any dimensionality similar to a variant of the Hamiltonian lattice model in field theory[25] already used in its Lagrangian version to simulate graphene.[26] In this model the electron's spin is strongly coupled to momentum and therefore the model is very reminiscent, in this respect, of the Wolff model of bismuth or lattice realizations of topological insulators. The lattice "regularization" is necessary to address the ultraviolet divergencies at the intermediated stages of calculations, a problem mentioned above. The universality of this description of Weyl fermions (of various origins) is supported by the fact that such a 2D model gives the same result for the interaction corrections as the tight-binding model on the honeycomb lattice with zero spin-orbit coupling.

In Sec. III the correction to the self-energy of a quasiparticle with momentum p is considered. It is shown that the Fermi velocity renormalization in 3D (already noted in Ref. 14) is logarithmic in the UV cutoff $\Lambda \sim \pi/a$ (a being the lattice spacing) very much like in 2D.[21] The velocity at normalization point $\overline{p}$ is

$$v_r(\overline{p}) \equiv \left.\frac{\varepsilon_{\mathbf{p}} + \Delta\varepsilon_{\mathbf{p}}}{p}\right|_{p=\overline{p}} = v\left[1 + \frac{2\alpha}{3\pi}\log\left(\frac{\hbar\Lambda}{\overline{p}}\right)\right]. \tag{4}$$

Section IV is devoted to a general derivation and application of the dynamical approach to the electric response to the dc and ac electric field. In particular, we obtain the slow current decay in a dc field E of the neutral, noninteracting 3D Weyl plasma and show that the relaxation is powerwise, see Fig. 1. The long time asymptotics is oscillating and depends on the microscopic details via cutoff a:

$$\frac{j_0(t)}{E} = \frac{N_W e^2}{12\pi^2\hbar v}\frac{1}{t}\left[1 + \cos\left(\frac{2vt}{a}\right)\right]. \tag{5}$$

Here N_W is the number of Weyl fermions. This explains how the pseudo-Ohmic dc conductivity vanishes in 3D. The relaxation dynamics therefore is qualitatively different from

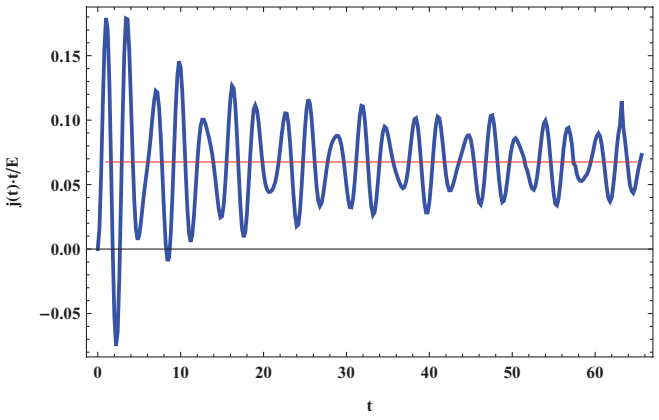

FIG. 1. (Color online) The response of the free Weyl semimetal to a dc electric field, multiplied by t, is shown as a function of time. The current's asymptotic value of zero is approached powerwise.

2D, where it is insensitive to the cutoff.[24] For the ac electric field similar slow convergence to the ac conductivity occurs, see Fig. 2. Even in the free Weyl semimetal one gets, in addition to a finite real (pseudodissipative) part linear in frequency,[14]

$$\sigma_0'(\Omega) = \frac{N_W e^2}{24\pi\hbar v}\Omega, \tag{6}$$

an imaginary part, logarithmically divergent as function of the UV cutoff:

$$\sigma_0''(\Omega) = -\frac{2}{\pi}\sigma_0'(\Omega)\log\frac{2\Lambda v}{\Omega}. \tag{7}$$

This is again different from graphene at zero doping and leads to important dielectric properties. Relaxation to the asymptotic behavior is faster at higher frequencies.

The leading interaction correction to the real and imaginary conductivities per Weyl point are the subject of Sec. V, see Fig. 3 for comparison with a metal and a semiconductor. The

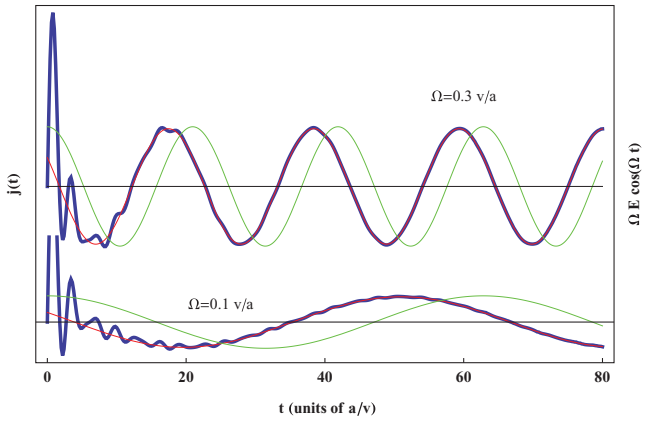

FIG. 2. (Color online) The response of the free Weyl semimetal to an ac electric field (green lines) is shown as a function of time for two different frequencies (magenta lines). The value of v/a is typically of order $\sim 3 \times 10^{15}$ Hz.

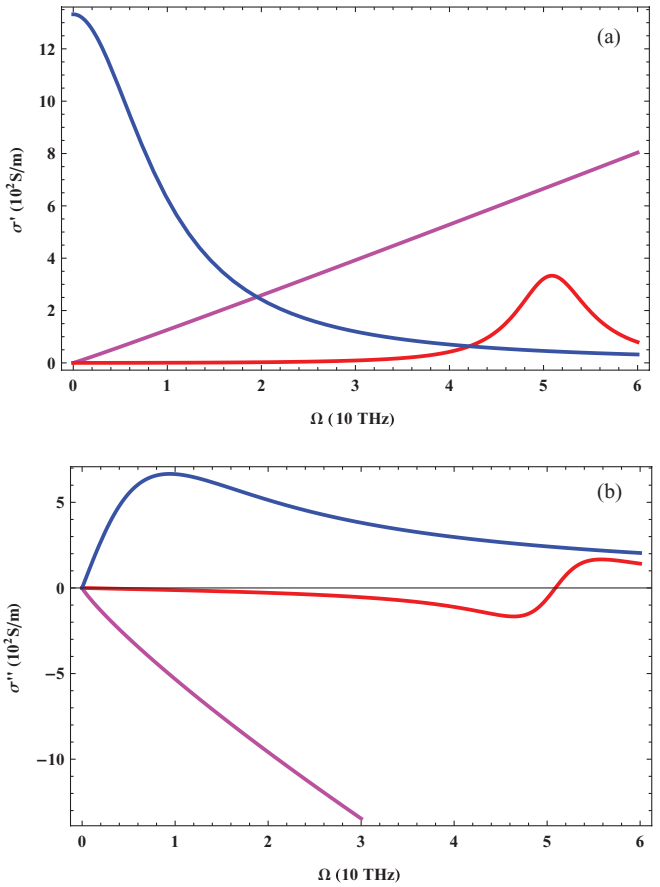

FIG. 3. (Color online) (a) The real part and (b) the imaginary part of the ac conductivity of the Weyl semimetal (magenta line) are compared with those of a band insulator (red line) and of a metal (blue line). The parameter values are given in the text.

result for the real part expressed via the renormalized Fermi velocity defined is still linear in frequency:

$$\sigma'(\Omega) = \sigma_0'(\Omega)\left[1 + \alpha\left(\frac{2}{3\pi}\log\frac{\Omega}{\overline{\Omega}} + C\right) + O(\alpha^2)\right],$$
$$C = -\frac{5}{3\pi} \approx -0.53. \tag{8}$$

The normalization frequency is $\overline{\Omega} = v\overline{p}/\hbar$. The imaginary part gets further logarithmically dependent on cutoff corrections,

$$\sigma''(\Omega) = \sigma_0''(\Omega)\left[1 + \frac{\alpha}{3\pi}\log\frac{2\Lambda v}{\Omega} + O(\alpha^2)\right], \tag{9}$$

despite an apparent "renormalizability" of the model to the leading order in α at least. The physical significance of the results including formulas including that for the complex dielectric constant, see Fig. 4, are summarized in the concluding Sec. VI. We speculate about obvious improvements like the random phase approximation, renormalization group, and a possibility of stronger coupling effects like the exciton condensation.

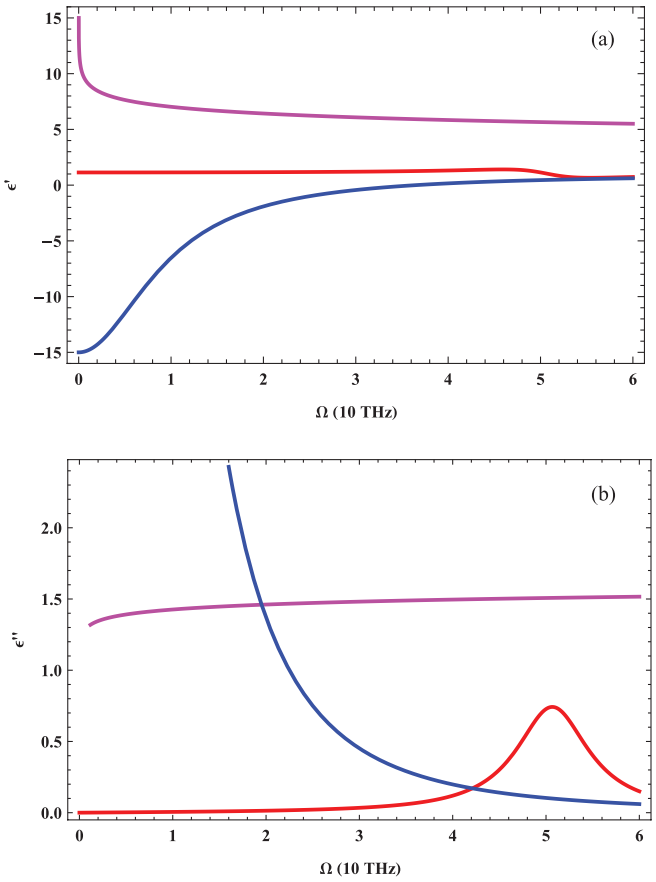

FIG. 4. (Color online) (a) The real part and (b) the imaginary part of the dielectric constant of the Weyl semimetal (magenta line) are compared with those of a band insulator (red line) and of a metal (blue line). The parameter values are given in the text.

II. TIGHT-BINDING MODEL WITH DOMINANT SPIN-ORBIT INTERACTIONS

A. Noninteracting Hamiltonian and linear response

The noninteracting tight-binding model is defined on the hypercubic lattice $\mathbf{n} = \sum_{i=1}^{3} n_i \mathbf{a}_i$ with lattice vectors $\mathbf{a}_i$ of length a by the Hamiltonian:

$$K_{\rm mc} = \frac{i}{2} \sum_{\mathbf{n},i} \Gamma_{\mathbf{n},i} c^{\dagger}_{\mathbf{n}} \sigma_i c_{\mathbf{n}+\mathbf{a}_i} + \text{H.c.} \tag{10}$$

Here σ_i are Pauli matrices, operators $c^{\alpha\dagger}_{\mathbf{n}}$ create a two-component spinor $\alpha = 1,2$, and $\Gamma_{\mathbf{n},i}$ is the hopping integral that in the presence of an external electromagnetic field, described by vector potential A_i, is

$$\Gamma_{\mathbf{n},i} = \gamma \exp\left[i \frac{ea}{c\hbar} \int_{s=0}^{1} A_i(\mathbf{n} + s\mathbf{a}_i, t) \right], \tag{11}$$

where the hopping energy γ is of order of the bandwidth. It is important to derive the current density directly in tight-binding model:

$$J_i(r,t) \equiv -c \frac{\partial K_{\rm mc}}{\partial A_i(\mathbf{r},t)} = \frac{ea}{2\hbar} \sum_n \int_{s=0}^{1} \delta^D(\mathbf{r} - \mathbf{n} - s\mathbf{a}_i) \Gamma_{\mathbf{n},i} c^{\dagger}_{\mathbf{n}} \sigma_i c_{\mathbf{n}+\mathbf{a}_i} + \text{H.c.} \tag{12}$$

It defines the UV regularization of the current operator that obeys the Ward identities. In linear response the current density operator is expanded up to the first order in $\mathbf{A}$ as $\mathbf{J} = \mathbf{J}_p + \mathbf{J}_d$:

$$J^p_i(\mathbf{r}) = \frac{ev}{2} \sum_n \Upsilon_n + \text{H.c.}, \tag{13}$$

$$J^d_i(\mathbf{r},t) = i \frac{e^2 v a}{2c\hbar} A_i(r,t) \sum_n \Upsilon_n + \text{H.c.}, \qquad \Upsilon_n = \int_{s=0}^{1} \delta^D(\mathbf{r} - \mathbf{n} - s\mathbf{a}_i)\, c^{\dagger}_{\mathbf{n}} \sigma_i c_{\mathbf{n}+\mathbf{a}_i}, \tag{14}$$

where $v = \gamma a/\hbar$. Space averages over volume $\mathcal{V}$ for a homogeneous vector potential $\mathbf{A}(t)$ simplify

$$j^p_i = \frac{1}{\mathcal{V}} \int_{\mathbf{r}} J^p_i(\mathbf{r}) = \frac{ev}{2\mathcal{V}} \sum_{\mathbf{n}} c^{\dagger}_{\mathbf{n}} \sigma_i c_{\mathbf{n}+\mathbf{a}_i} + \text{H.c.}, \qquad j^d_i = \frac{1}{\mathcal{V}} \int_{\mathbf{r}} J^d_i(\mathbf{r},t) = i \frac{e^2 a v}{2c\hbar\mathcal{V}} A_i(t) \sum_{\mathbf{n}} c^{\dagger}_{\mathbf{n}} \sigma_i c_{\mathbf{n}+\mathbf{a}_i} + \text{H.c.} \tag{15}$$

Expansion of the minimally coupled Hamiltonian in electric field is

$$K_{\rm mc} \approx K + H_{\rm ext}, \quad H_{\rm ext} = -\frac{1}{c} \int_{\mathbf{r}} \mathbf{J}^p \cdot \mathbf{A}(t). \tag{16}$$

Defining Fourier components by $c^{\alpha}_{\mathbf{n}} = \mathcal{N}^{-1/2} \sum_{\mathbf{k}} e^{-i\mathbf{k}\cdot\mathbf{n}} c^{\alpha}_{\mathbf{k}}$, where the number of unit cells is $\mathcal{N} = \mathcal{V}/a^D$, one has

$$K = \gamma \sum_{\mathbf{k},i} \sin(k_i a) c^{+}_{\mathbf{k}} \sigma_i c_{\mathbf{k}}. \tag{17}$$

Diagonalization of K is achieved by adopting a reinterpretation of the absence of an electron in the valence band as a hole and using units $\hbar = a = v = 1$ by

$$c^{\alpha}_{\mathbf{k}} = v^{\alpha}_{\mathbf{k}} a_{\mathbf{k}} + u^{\alpha}_{\mathbf{k}} b^{+}_{-\mathbf{k}} \to c^{\alpha+}_{\mathbf{k}} = v^{\alpha *}_{\mathbf{k}} a^{+}_{\mathbf{k}} + u^{\alpha *}_{\mathbf{k}} b_{-\mathbf{k}}, \tag{18}$$

with spinors $v_{\mathbf{k}}$ and $u_{\mathbf{k}}$ given in Appendix A. Up to an additive constant it becomes

$$K = \sum_{\mathbf{k}} \varepsilon_{\mathbf{k}} (a^{+}_{\mathbf{k}} a_{\mathbf{k}} + b^{+}_{\mathbf{k}} b_{\mathbf{k}}), \tag{19}$$

where

$$\varepsilon_{\mathbf{k}} = \sqrt{\widehat{k}_1^{\,2} + \widehat{k}_2^{\,2} + \widehat{k}_3^{\,2}}, \tag{20}$$

and the notation $\widehat{k} \equiv \sin k$ was introduced. In 3D one observes eight Weyl points at which $\varepsilon_{\mathbf{k}} = 0$ inside the Brillouin zone (BZ). Four are right handed: one in the center (the Γ point) and three on the faces (X), while four are left handed: three on the edges (M) and one in the corner (R). The chirality is determined by the expansion of the Hamiltonian Eq. (17) around a Weyl point $\mathbf{W}$, $\text{sgn}(\varepsilon_{ijk} Q^1_i Q^2_j Q^3_k)$, where $\mathbf{Q}^i = \frac{\partial}{\partial \mathbf{k}} \widehat{k}_i |_{\mathbf{W}}$. Similarly, in 2D one has two right handed Weyls at Γ and R and two left handed at M.

The paramagnetic and diamagnetic parts of the current due to an electric field (along, let us say, the z direction), $\mathbf{A}(t) = (0,0,A(t))$; $E(t) = -c\frac{d}{dt}A(t)$, are

$$j^p = \frac{e}{\mathcal{V}}\sum_{\mathbf{k}}[\iota_{\mathbf{k}}(a^+_{\mathbf{k}}a_{\mathbf{k}} + b^+_{-\mathbf{k}}b_{-\mathbf{k}}) + i\chi_{\mathbf{k}}b_{-\mathbf{k}}a_{\mathbf{k}}] + \text{H.c.},$$
$$j^d = \frac{e^2}{\mathcal{V}}A(t)\sum_{\mathbf{k}}\frac{\widehat{k}_z}{\varepsilon_{\mathbf{k}}}\Big[\frac{\widehat{k}_z}{2}(a^+_{\mathbf{k}}a_{\mathbf{k}} + b^+_{-\mathbf{k}}b_{-\mathbf{k}}) - (\widehat{k}_x + i\widehat{k}_y)b_{-\mathbf{k}}a_{\mathbf{k}}\Big] + \text{H.c.}, \quad (21)$$

where the functions $\chi_{\mathbf{k}}$ and $\iota_{\mathbf{k}}$ are defined in Appendix A.

B. Coulomb interaction

Using the expression for the particle densities in momentum space (Einstein summation implied for spins only):

$$N_{\mathbf{n}} = c^{\alpha\dagger}_{\mathbf{n}}c^{\alpha}_{\mathbf{n}} = \mathcal{N}^{-1}\sum_{\mathbf{kl}}e^{i(\mathbf{l}-k)\cdot\mathbf{n}}c^{\alpha+}_{\mathbf{l}}c^{\alpha}_{\mathbf{k}}, \quad (22)$$

the Coulomb interaction takes the form

$$V = \frac{1}{2}\sum_{\mathbf{nm}}\frac{e^2}{|\mathbf{n}-\mathbf{m}|}N_{\mathbf{n}}N_{\mathbf{m}} = \sum_{\mathbf{klk'l'}}v_{\mathbf{klk'l'}}c^{\alpha+}_{\mathbf{l}}c^{\alpha}_{\mathbf{k}}c^{\alpha'+}_{\mathbf{l'}}c^{\alpha'}_{\mathbf{k'}}, \quad (23)$$

$$v_{\mathbf{klk'l'}} = \frac{1}{2\mathcal{V}}\sum_{\mathbf{p}}v_{\mathbf{p}}\delta_{\mathbf{l}-\mathbf{k}-\mathbf{p}}\delta_{\mathbf{l'}-\mathbf{k'}+\mathbf{p}}, \quad (24)$$

with Fourier transform of the interaction being $v_{\mathbf{p}} = \frac{4\pi e^2}{a^2\mathbf{p}^2}$. It is important to note that the electric charge of the effective tight-binding model should include the contributions to the screening due to the polarization constant ϵ caused by degrees of freedom not included in the model, so the "bare" charge includes this effect $e^2 = e^2_{\text{el}}/\epsilon$. We require charge neutrality that is achieved by leaving out all the contributions including $v_{\mathbf{p}=\mathbf{0}}$. This prescription is always implied in what follows. It is convenient to normal order V with respect to operators a and b diagonalizing the "kinetic" term K via Eq. (18):

$$V = V^{40} + V^{31} + V^{22} + V^{13} + V^{04} + V^{11}, \quad (25)$$

where the part V^{ij} contains i creation operators a^+ or b^+ and j annihilation operators a or b, all specified in Appendix A. In principle, the quadratic pair creation V^{20} and the pair annihilation terms V^{02} could have appeared. The fact that they have not, explained in Appendix A, greatly simplifies the calculation and makes it competitive (at least to the leading order) with the diagrammatic approach. The "time independent" approach is however much more transparent, when one realizes that excitations can be created in fours rather than in pairs in this particular model.

III. QUASIPARTICLES AND RENORMALIZATION OF THE FERMI VELOCITY

The energy of an electron above the Fermi level with quasimomentum $\mathbf{p}$, $|\mathbf{p}\rangle = a^+_{\mathbf{p}}|0\rangle$, in the noninteracting model described by the Hamiltonian Eq. (19) is

$$\langle\mathbf{p}|K|\mathbf{p}\rangle = \langle 0|a_{\mathbf{p}}\sum_{\mathbf{l}}\varepsilon_{\mathbf{l}}(a^+_{\mathbf{l}}a_{\mathbf{l}} + b^+_{\mathbf{l}}b_{\mathbf{l}})a^+_{\mathbf{p}}|0\rangle = \varepsilon_{\mathbf{p}}. \quad (26)$$

The interaction correction is

$$\Delta\varepsilon_{\mathbf{p}} = \langle\mathbf{p}|V|\mathbf{p}\rangle = \langle 0|a_{\mathbf{p}}Va^+_{\mathbf{p}}|0\rangle. \quad (27)$$

Obviously only contributions with equal numbers of creation and annihilation operators V^{22} and V^{11} can contribute. The first term contains (see Appendix A) a^+b^+ab, b^+b^+bb, and a^+a^+aa terms, of which only the last one could contribute to the expectation value Eq. (27), yet it vanishes:

$$\Delta\varepsilon^{22}_{\mathbf{p}} = -\sum_{\mathbf{klk'l'}}v_{\mathbf{klk'l'}}(v^*_{\mathbf{l'}}\cdot v_{\mathbf{k'}})(v^*_{\mathbf{l}}\cdot v_{\mathbf{k}})\langle 0|a_{\mathbf{p}}a^+_{\mathbf{l}}a^+_{\mathbf{l'}}a_{\mathbf{k}}a_{\mathbf{k'}}a^+_{\mathbf{p}}|0\rangle$$
$$= -\sum_{\mathbf{kll'}}v_{\mathbf{klpl'}}(v^*_{\mathbf{l'}}\cdot v_{\mathbf{p}})(v^*_{\mathbf{l}}\cdot v_{\mathbf{k}})\langle 0|a_{\mathbf{p}}a^+_{\mathbf{l}}a^+_{\mathbf{l'}}a_{\mathbf{k}}|0\rangle = 0. \quad (28)$$

We are left with the simple quadratic part V^{11}:

$$\Delta\varepsilon^{11}_{\mathbf{p}} = \frac{1}{2}\sum_{\mathbf{ql}}v_{\mathbf{l}-\mathbf{q}}g_{\mathbf{ql}}\langle 0|a_{\mathbf{p}}(a^+_{\mathbf{l}}a_{\mathbf{l}} + b^+_{-\mathbf{l}}b_{-\mathbf{l}})a^+_{\mathbf{p}}|0\rangle$$
$$= \frac{1}{2}\sum_{\mathbf{q}}v_{\mathbf{p}-\mathbf{q}}g_{\mathbf{qp}}, \quad (29)$$

where

$$g_{\mathbf{pq}} \equiv |v^*_{\mathbf{q}}\cdot v_{\mathbf{p}}|^2 - |u^*_{\mathbf{q}}\cdot v_{\mathbf{p}}|^2. \quad (30)$$

This results in

$$\Delta\varepsilon_{\mathbf{p}} = \frac{e^2p}{3\pi}\Big[\log\frac{3\pi^2}{2a^2p^2} + O(p^2)\Big]. \quad (31)$$

It is instructive to estimate it using the expansion around any of the eight Weyl points with the momenta restricted, say, by $q < \Lambda < \pi/2a$, thus omitting some contributions far from the Weyl points that innocently could be thought to be small, but, as the graphene example taught us, might become perfidious if powerwise UV divergencies appear in the intermediate stages of the calculation. In the present case divergencies are just logarithmic though and one proceeds by expanding around one of the Weyl points,

$$g_{\mathbf{pq}} \approx \cos\theta_{\mathbf{q}}\cos\theta_{\mathbf{p}} + \sin\theta_{\mathbf{q}}\sin\theta_{\mathbf{p}}\cos(\phi_{\mathbf{p}} - \phi_{\mathbf{q}}), \quad (32)$$

where spherical coordinates $\mathbf{q} = q(\sin\theta_{\mathbf{q}}\cos\phi_{\mathbf{q}}, \sin\theta_{\mathbf{q}}\sin\phi_{\mathbf{q}}, \cos\theta_{\mathbf{q}})$ were used. The sum is transformed into an integral:

$$\Delta\varepsilon^{11}_{\mathbf{p}} = \frac{e^2}{2(2\pi)^3}\int_{q\phi_{\mathbf{q}}\theta_{\mathbf{q}}}\frac{4\pi\sin\theta_{\mathbf{q}}q^2g_{\mathbf{pq}}}{p^2+q^2-2pqg_{\mathbf{pq}}}. \quad (33)$$

The integrals over angles can be performed, see Appendix B, resulting in [for $\mathbf{p} = p(1,0,0)$]

$$\Delta\varepsilon^{11}_{\mathbf{p}} = \frac{e^2}{4\pi}\int_{q=0}^{\Lambda}\Big[\frac{1+r^2}{2}\log\Big(\frac{1+r}{1-r}\Big)^2 - 2r\Big], \quad (34)$$

where $r = q/p$. Changing variables in the remaining integral establishes the leading linear dependence on p:

$$\Delta\varepsilon_{\mathbf{p}} = \frac{e^2 p}{4\pi}\int_{r=0}^{\Lambda/p}\left[\frac{1+r^2}{2}\log\left(\frac{1+r}{1-r}\right)^2 - 2r\right] = \frac{e^2 p}{3\pi}\left[\log\left(\frac{\Lambda^2}{p^2}\right) + \frac{5}{3}\right]. \quad (35)$$

Comparing with the exact result for the "universal" model, Eq. (31), we can choose the value of the cutoff to be slightly outside of the continuum model applicability range $\Lambda = 0.53\frac{\pi}{a}$. This means that the continuum model cannot determine correctly the constant term that is model dependent. To summarize, one indeed observes just a logarithmic divergence and therefore can renormalize the Fermi velocity written in physical units in Eq. (4).

In 2D the corresponding calculation gives a well known "running" of the graphene velocity towards higher velocities.[21] Therefore the running of the Fermi velocity in Weyl semimetal is very much like in (undoped) graphene.

IV. DYNAMICS OF ELECTRIC RESPONSE: CURRENT DECAY IN DC FIELD AND INDUCTIVE RESPONSE IN AC FIELD OF THE NONINTERACTING WEYL FERMIONS NEUTRAL PLASMA

In this section we first calculate the time evolution of the current when the external electric field is switched on in order to obtain the dc and ac electric response. This is done however within a "time independent" formalism to carefully trace the states that contribute to the dynamics and investigate the emergence of the steady state.

A. The electric current evolution within linear response

We use the dynamical approach[22] to the semimetal response rather than the more customary diagrammatic method not just to investigate dynamics under dc or ac field, but also to clarify several fundamental issues in the following sections concerning the Coulomb interaction corrections to the ac conductivity. First the nature of the dependence of the physical quantities on the UV "cutoff" $1/a$ (renormalization) is elucidated, next the time evolution is exploited to demonstrate the inductive response of the 3D semimetal even without electron-electron interaction and contrast it with the purely pseudo-Ohmic response of graphene.

The paramagnetic contribution in the Heisenberg picture is given by the vacuum expectation value (VEV):

$$\langle \mathbf{J}^p(\mathbf{r})\rangle = \langle\psi_{\rm mc}(t)|\mathbf{J}^p(\mathbf{r})|\psi_{\rm mc}(t)\rangle = \langle\psi(0)|U_{\rm mc}^{-1}(t)\mathbf{J}^p(\mathbf{r})U_{\rm mc}(t)|\psi(0)\rangle. \quad (36)$$

The ground state $\psi(0)$ is that of an interacting electron system without the external field. Expanding to "linear response" in coupling to the external electric field (considered homogeneous and oriented along the z direction), Eq. (16),

$$U_{\rm mc}(t) = U_K(t)\left[1 - i\int_{t_1=0}^{t} U_H^{-1}(t_1)H_{\rm ext}(t_1)U_H(t_1)\right], \quad (37)$$

where $U_H(t) = e^{-i(K+V)t}$, one gets

$$\langle \mathbf{J}^p(\mathbf{r},t)\rangle = i\int_{t_1=0}^{t} A(t_1)\int_{r'}\langle\psi(0)|e^{iHt}J_z^p(\mathbf{r})e^{-iH(t-t_1)}\mathbf{J}^p \times(\mathbf{r}')e^{-iHt_1}|\psi(0)\rangle + \text{c.c.} \quad (38)$$

The diamagnetic current, Eq. (13), is already of the first order in electric field. In the next section the full model including the many-body effects will be considered. In this section we neglect the interaction V to solve exactly for the time evolution of the current density.

B. Time dependence of the current generated by a time dependent electric field

In the absence of the Coulomb interaction the VEV of the average paramagnetic current density [in the field direction z, see Eq. (13)] takes a form

$$\left\langle j_0^p(t)\right\rangle = i\mathcal{V}\int_{t_1=0}^{t} A(t_1)\langle 0|e^{iKt}j^p e^{-iK(t-t_1)}j^p e^{-iKt_1}|0\rangle + \text{c.c.} \quad (39)$$

Using definitions of the tight-binding Hamiltonian and the current density operator, Eqs. (19) and (21), one obtains

$$\left\langle j_0^p(t)\right\rangle = \frac{e^2}{\mathcal{V}}\int_{t_1=0}^{t} A(t_1)\sum_{\mathbf{k}}|\chi_{\mathbf{k}}|^2\sin[2\varepsilon_{\mathbf{k}}(t-t_1)]. \quad (40)$$

Similarly the diamagnetic contribution, using Eq. (21), is

$$\left\langle j_0^d(t)\right\rangle = \langle 0|j^d|0\rangle = -\frac{e^2}{\mathcal{V}}A(t)\sum_{\mathbf{k}}\frac{\widehat{k}_z^2}{\varepsilon_k}. \quad (41)$$

To continue one has to specify the time dependence of the applied electric field. We start in the next subsection with the constant electric field and then continue to the ac case.

C. Decay of current in the dc electric field

In the homogeneous dc electric field described by the vector potential $A(t) = -cEt$, one obtains from Eq. (40) the average current. The integral over t_1 results in

$$\frac{j_0(t)}{E} = \frac{e^2}{\mathcal{V}}\sum_{\mathbf{k}}\left\{t\frac{\widehat{k}_z^2}{\varepsilon_{\mathbf{k}}} - |\chi_{\mathbf{k}}|^2\left[\frac{t}{2\varepsilon_{\mathbf{k}}} - \frac{\sin(2\varepsilon_{\mathbf{k}}t)}{4\varepsilon_{\mathbf{k}}^2}\right]\right\}. \quad (42)$$

One expects that the neutral plasma system that does not possess electric charges on the Fermi level will not have the "acceleration" terms linear in time t that appear in the above equation. Indeed the sum of the first two terms vanishes:

$$\frac{j_0^{\rm acc}(t)}{E} = -t\frac{e^2}{\mathcal{V}}\sum_{\mathbf{k}}\left[\varepsilon_{\mathbf{k}}^{-3}\left(1-\widehat{k}_z^2\right)\left(\widehat{k}_x^2+\widehat{k}_y^2\right) + \varepsilon_{\mathbf{k}}^{-1}\widehat{k}_z^2\right] = 0. \quad (43)$$

This is seen as follows. The integral over the BZ can be represented as an integral over the full $\frac{d}{dk_z}$ derivative like in graphene.[22] Since the BZ can be taken periodically in the quasimomentum component k_z, the integral over the derivative vanishes. The physical arguments put forward in the framework of graphene[20] in order to comprehend this

apply equally well here and are not repeated. The remaining nonaccelerating part,

$$\frac{j_0(t)}{E} = \frac{e^2}{2\mathcal{V}} \sum_{\mathbf{k}} \varepsilon_{\mathbf{k}}^{-4} \left(1-\widehat{k}_z^2\right)\left(\widehat{k}_x^2+\widehat{k}_y^2\right) \sin(2\varepsilon_{\mathbf{k}} t), \quad (44)$$

is presented in Fig. 1. It decays as given (in physical units) in Eq. (5), exhibiting the zero conductivity rather than a universal finite value as in graphene. This asymptotic value of zero is approached therefore powerwise and oscillating. Note the dependence on the ultraviolet cutoff that did not appear in graphene.[24]

D. Universal dissipative and nonuniversal inductive response to the ac electric field

The ac electric field $E\cos(\Omega t)$ is represented by the oscillating vector potential $A(t) = -\frac{cE}{\Omega}\sin(\Omega t)$. The "universal" nearest neighbors tight-binding model is relevant only for frequencies Ω smaller than the hopping integral $\gamma/\hbar$. However, as we noticed in the context of graphene,[20] the use of the expansion of the dispersion relation near the Weyl points should be done with some care.

Performing the integral over t_1 in Eq. (40), one now obtains the current:

$$\frac{j_0(t)}{E} = \frac{e^2}{\mathcal{V}\Omega} \sum_{\mathbf{k}} \left\{ \varepsilon_{\mathbf{k}}^{-1} \widehat{k}_3^2 \sin(\Omega t) - 2\varepsilon_{\mathbf{k}}^{-2}\left(1-\widehat{k}_z^2\right)\left(\widehat{k}_x^2+\widehat{k}_y^2\right) \times \frac{\Omega\sin(2\varepsilon_{\mathbf{k}} t) - 2\varepsilon_{\mathbf{k}}\sin(\Omega t)}{\Omega^2 - 4\varepsilon_{\mathbf{k}}^2} \right\}. \quad (45)$$

As in graphene, it is very difficult to approach frequencies of interest $\Omega \ll \gamma/\hbar$, when the conductivity is presented in this form. However it becomes substantially simpler numerically when one subtracts the vanishing acceleration term Eq. (43) that we have encountered in the dc calculation, with t replaced by $1/\Omega$:

$$\frac{j_0(t)}{E} = \frac{e^2}{\mathcal{V}} \sum_{\mathbf{k}} \varepsilon_{\mathbf{k}}^{-3}\left(1-\widehat{k}_z^2\right)\left(\widehat{k}_x^2+\widehat{k}_y^2\right) \times \frac{\Omega\sin(\Omega t) - 2\varepsilon_{\mathbf{k}}\sin(2\varepsilon_{\mathbf{k}} t)}{\Omega^2 - 4\varepsilon_{\mathbf{k}}^2}. \quad (46)$$

This is shown (together with the electric field) in Fig. 2 for two values of frequency. One observes that beyond a certain relaxation time the response becomes periodic, exhibiting a phase difference between the current (points) and the electric field (solid lines). To obtain the steady state value of the complex conductivity we average over time with a damping factor η using

$$\sigma(\Omega) = \lim_{\eta\to 0+} \frac{2\eta}{E} \int_{t=0}^{\infty} e^{i\Omega t - \eta t} j(t). \quad (47)$$

The time integration in Eq. (46) with the current density of Eq. (46) results in

$$\sigma_0(\Omega) = -\frac{ie^2\Omega}{\mathcal{V}} \sum_{\mathbf{k}} \varepsilon_{\mathbf{k}}^{-3}\left(1-\widehat{k}_z^2\right)\left(\widehat{k}_x^2+\widehat{k}_y^2\right) \frac{1}{4\varepsilon_{\mathbf{k}}^2 - \Omega_+^2}, \quad (48)$$

where $\Omega_+ \equiv \Omega + i\eta$. Due the the factor $\varepsilon_{\mathbf{k}}^3$ in the denominator one might worry about infrared divergences at the Weyl points, but as we see below, when the neighborhood of these points is investigated, there are no such divergences and one just has to handle the threshold singularity at $\varepsilon_{\mathbf{k}} = \Omega_+/2$. The exact integral is given (in physical units) in Eqs. (6) and (7) with $\Lambda = 0.37\frac{\pi}{a}$, where a is the lattice spacing. To avoid the threshold singularity we also calculated the Matsubara conductivity for $\Omega = -i\omega$:

$$\sigma_{M0}(\omega) = \frac{e^2\omega}{\mathcal{V}} \sum_{\mathbf{k}} \varepsilon_{\mathbf{k}}^{-3}\left(1-\widehat{k}_z^2\right)\left(\widehat{k}_x^2+\widehat{k}_y^2\right) \frac{1}{4\varepsilon_{\mathbf{k}}^2 + \omega^2} = \frac{e^2\omega}{3\pi^2}\log\frac{4\Lambda^2}{\omega^2}. \quad (49)$$

This can be extended to finite temperature via the Matsubara substitution $\omega \to \omega + \pi k_B T/\hbar$; the dc conductivity at finite temperature thus becomes

$$\sigma_{\rm dc}(T) = \frac{e^2 T}{3\pi^2}\log\left(\frac{4\Lambda^2}{\pi^2 T^2}\right). \quad (50)$$

It is important to note that both the imaginary part and the temperature dependence of the dc conductivity are logarithmically divergent as a function of the UV cutoff. Therefore these *physical* quantities are sensitive to the microscopic model even before one considers interactions between electrons. These quantities cannot be absorbed by renormalization due to interactions (see Sec. V) and its interpretation is proposed in Sec. VI.

Now we proceed to try to use the continuum model near the Weyl points. After the subtraction of "anomalous" acceleration terms most of the contributions for $\Omega \ll \gamma/\hbar$ come from the immediate neighborhoods of the Weyl points.[22] Due to symmetries it suffices to consider one of them. The neighborhood of the origin will be defined by $k < \Lambda < \pi/2$. Here two differences emanate compared to the transport in graphene. In graphene the lattice spacing is irrelevant, so that the conductivity can be calculated within the continuum Weyl model and the ac conductivity is real for all frequencies $\Omega \ll \gamma/\hbar$. In the present case an inductive part appears and moreover depends logarithmically on the lattice spacing. To see this explicitly, let us calculate the ac conductivity approximately by using the Weyl approximation (linearization of the dispersion relation) for the contribution of the Weyl points. Within the continuum approximation in spherical coordinates one writes the sum in Eq. (48) as

$$\sigma_0(\Omega) = -\frac{8ie^2}{(2\pi)^3}\int_{k=0}^{\Lambda} k \int_{\theta,\phi} \sin^3\theta \frac{\Omega}{4k^2-\Omega_+^2} = -\frac{32e^2\Omega}{3(2\pi)^2}\int_{k=0}^{\Lambda}\frac{k}{4k^2-\Omega_+^2}, \quad (51)$$

where the factor 8 is due to the multiplicity of the Weyl points in our "universal" tight-binding model. The integration over k finally gives

$$\sigma_0(\Omega) = \frac{e^2\Omega}{3\pi}\left(1 - \frac{i}{\pi}\log\frac{4\Lambda^2-\Omega^2}{\Omega^2}\right) \approx \frac{e^2\Omega}{3\pi} - i\frac{e^2\Omega}{3\pi^2}\log\frac{4\Lambda^2}{\Omega^2}. \quad (52)$$

In the last line small terms of the relative order Ω^2/Λ^2 were omitted. The finite result for the real part and regularized Matsubara conductivity were first obtained in Ref. 14.

Let us emphasize that the electric properties in 3D differ from that in 2D (graphene) in that there appears an imaginary part of conductivity that is of the same size and sometimes even larger than the pseudodissipative one. Now we turn to the study of the many-body effects in 3D Weyl semimetal.

V. THE INTERACTION CORRECTION TO THE AC CONDUCTIVITY OF THE WEYL SEMIMETAL

A. Leading corrections to the current evolution in a time dependent field

The expressions for the diamagnetic and the paramagnetic components of the current density as a linear response to arbitrarily time dependent electric fields are given by Eqs. (13) and (38), respectively. The evolution operator however should be modified as

$$e^{-i(K+V)t} = e^{-iKt}\left[1 - i\int_{\tau=0}^{t} e^{iK\tau} V e^{-iK\tau} + O(V^2)\right], \quad (53)$$

and the ground state (at initial time or Schrödinger) as

$$|\psi(0)\rangle = |0\rangle + |\psi_1\rangle, \quad |\psi_1\rangle = -\frac{1}{K} V^{(4,0)}|0\rangle, \quad (54)$$

with the correction to energy being $\Delta E = \langle 0|V|0\rangle = 0$ since the constant term in the energy will be consistently omitted after the Hamiltonian was normal ordered. Only creation of four particles at once is possible within the universal model, as is shown in Appendix B. The pair creating part $V^{(2,0)}$ vanishes. This simplifies the problem significantly. For example, the diamagnetic component is absent due to this. Indeed the diamagnetic current is quadratic [Eq. (13)] and hence the correction

$$\begin{aligned}\Delta j^d(t) &= \langle\psi_1|e^{-iKt} j^d e^{iKt}|0\rangle + \text{c.c.}\\ &= \langle\psi_1|j^d|0\rangle + \text{c.c.} = 0.\end{aligned} \quad (55)$$

The paramagnetic correction [in homogeneous electric field along certain direction described by vector potential $A(t)$] of Eq. (38) in the presence of Coulomb interactions takes a form

$$\begin{aligned} j^p(t) &= -ie^2\int_{t_1=0}^{t} A(t_1)\Xi(t-t_1) + \text{c.c.},\\ \Xi(t-t_1) &= \langle\psi(0)|e^{iHt} j^p e^{-iH(t-t_1)} j^p e^{-iHt_1}|\psi(0)\rangle\\ &= \langle\psi(0)|j^p e^{-iH(t-t_1)} j^p|\psi(0)\rangle. \end{aligned} \quad (56)$$

Expanding in interaction with help of Eqs. (53) and (54), the correction to the expectation value in the interacting ground state Ξ above in terms of the unperturbed vacuum expectation values is

$$\begin{aligned}&\Delta\Xi(t-t_1)\\ &= -i\langle 0|j^p\int_{\tau=0}^{t-t_1} e^{-iK(t-t_1-\tau)}(V^{(1,1)}+V^{(2,2)})e^{-iK\tau} j^p|0\rangle\\ &\quad -\langle 0|j^p e^{-iK(t-t_1)} j^p \frac{1}{K} V^{(4,0)}|0\rangle\\ &\quad -\langle 0|V^{(0,4)}\frac{1}{K} j^p e^{-iK(t-t_1)} j^p|0\rangle. \end{aligned} \quad (57)$$

The other contributions vanish, again due to absence of pair creations at this order. The first term corresponds to the fermion self-energy correction, while the rest describe the vertex correction. These are readily calculated:

$$\begin{aligned}\Delta j(t) = \frac{e^2}{\mathcal{V}^2}\int_{t_1=0}^{t} A(t_1)\sum_{\mathbf{pq}} v_{\mathbf{p}-\mathbf{q}}\Big\{&(t-t_1)\cos[2\varepsilon_{\mathbf{q}}(t-t_1)]\\ &\times|\chi_{\mathbf{q}}|^2 g_{\mathbf{qp}} + g^{-}_{\mathbf{qp}}\frac{\sin[2\varepsilon_{\mathbf{q}}(t-t_1)]}{\varepsilon_{\mathbf{q}}+\varepsilon_{\mathbf{p}}}\\ &+\frac{1}{2}g^{+}_{\mathbf{qp}}\frac{\sin[2\varepsilon_{\mathbf{p}}(t-t_1)]-\sin[2\varepsilon_{\mathbf{q}}(t-t_1)]}{\varepsilon_{\mathbf{q}}-\varepsilon_{\mathbf{p}}}\Big\}, \end{aligned} \quad (58)$$

where $g_{\mathbf{qp}}$ is defined in Eq. (30) and

$$g^{-}_{\mathbf{qp}} = \text{Re}[\chi^*_{\mathbf{q}}\chi^*_{\mathbf{p}}(u^*_{\mathbf{p}}\cdot v_{\mathbf{q}})^2], \quad g^{+}_{\mathbf{qp}} = \text{Re}[\chi_{\mathbf{q}}\chi^*_{\mathbf{p}}(v^*_{\mathbf{q}}\cdot v_{\mathbf{p}})^2]. \quad (59)$$

This can be calculated using the same methods as in the leading order in the previous section. The dc conductivity correction vanishes linearly. Finally we calculate the correction to current for the ac electric field.

B. Correction to the ac conductivity

In the homogeneous ac electric field, $A(t) = -\frac{cE}{\Omega}\sin(\Omega t)$, the ac conductivity averaged over time as in the leading order [Eq. (47)] is

$$\begin{aligned}\sigma_1(\Omega) = \frac{2ie^2}{\mathcal{V}^2\Omega}\sum_{\mathbf{pq}}\frac{v_{\mathbf{p}-\mathbf{q}}}{4\varepsilon_{\mathbf{q}}^2-\Omega_+^2}\Big[&-\frac{|\chi_{\mathbf{q}}|^2 g_{\mathbf{qp}}\left(4\varepsilon_{\mathbf{q}}^2+\Omega^2\right)}{4\varepsilon_{\mathbf{q}}^2-\Omega_+^2}\\ &+\frac{2g^{-}_{\mathbf{qp}}\varepsilon_{\mathbf{q}}}{\varepsilon_{\mathbf{q}}+\varepsilon_{\mathbf{p}}}+\frac{g^{+}_{\mathbf{qp}}(4\varepsilon_{\mathbf{q}}\varepsilon_{\mathbf{p}}+\Omega^2)}{4\varepsilon_{\mathbf{p}}^2-\Omega_+^2}\Big], \end{aligned} \quad (60)$$

where $\Omega_+ \equiv \Omega + i\eta$. Subtracting the dc limit (that vanishes after averaging over time) like in the leading order, one obtains a much more converging expression proportional to the frequency

$$\begin{aligned}\sigma_1(\Omega) = \frac{ie^2\Omega}{2\mathcal{V}^2}\sum_{\mathbf{pq}}\frac{v_{\mathbf{p}-\mathbf{q}}}{4\varepsilon_{\mathbf{q}}^2-\Omega_+^2}\Big[&-\frac{|\chi_{\mathbf{q}}|^2 g_{\mathbf{qp}}\left(12\varepsilon_{\mathbf{q}}^2-\Omega^2\right)}{\varepsilon_{\mathbf{q}}^2\left(4\varepsilon_{\mathbf{q}}^2-\Omega_+^2\right)}\\ &+\frac{2g^{-}_{\mathbf{qp}}}{\varepsilon_{\mathbf{q}}(\varepsilon_{\mathbf{q}}+\varepsilon_{\mathbf{p}})}+\frac{g^{+}_{\mathbf{qp}}\left(4\varepsilon_{\mathbf{q}}\varepsilon_{\mathbf{p}}+4\varepsilon_{\mathbf{q}}^2+4\varepsilon_{\mathbf{p}}^2-\Omega^2\right)}{\varepsilon_{\mathbf{q}}\varepsilon_{\mathbf{p}}\left(4\varepsilon_{\mathbf{p}}^2-\Omega_+^2\right)}\Big]. \end{aligned} \quad (61)$$

The numerical evaluation results in (without subleading terms in the imaginary part)

$$\sigma_1(\Omega) = \frac{e^4\Omega}{9\pi^2}\left[-\log\frac{\pi^2}{a^2\Omega^2} - 5 + \frac{i}{8\pi}\log^2\frac{\pi^2}{a^2\Omega^2}\right]. \quad (62)$$

It is however instructive to obtain this expression within the continuum (Weyl) approximation valid within radius Λ around each of the eight Weyl points.

Near a Weyl point one has the following expansion of the functions appearing in Eq. (61) in spherical coordinates around one of the points (chosen to be the origin Γ):

$$\chi_{\mathbf{k}} = -ie^{i\phi_{\mathbf{k}}}\sin\theta_{\mathbf{k}}, \quad (63)$$

$$\begin{aligned}g^{\pm}_{\mathbf{qp}} = \tfrac{1}{2}\sin\theta_{\mathbf{q}}\sin\theta_{\mathbf{p}}[&\cos(\phi_{\mathbf{q}}-\phi_{\mathbf{p}})(\cos\theta_{\mathbf{q}}\cos\theta_{\mathbf{p}}\pm 1)\\ &+\sin\theta_{\mathbf{q}}\sin\theta_{\mathbf{p}}], \end{aligned} \quad (64)$$

complementing Eq. (32) for $g_{\mathbf{qp}}$. The sum and the Coulomb potential in Eq. (61) are written as

$$\frac{8}{2(2\pi)^6}\int_{pq\phi_{\mathbf{p}}\phi_{\mathbf{q}}\theta_{\mathbf{p}}\theta_{\mathbf{q}}} \times \frac{4\pi p^2 q^2 \sin\theta_{\mathbf{p}} \sin\theta_{\mathbf{q}}}{p^2+q^2-2pq[\cos\theta_{\mathbf{p}}\cos\theta_{\mathbf{q}} + \sin\theta_{\mathbf{p}}\sin\theta_{\mathbf{q}}\cos(\phi_{\mathbf{p}}-\phi_{\mathbf{q}})]}. \tag{65}$$

The integrals over all the angles can be performed, see Appendix B,

$$\sigma_1(\Omega) = \frac{2ie^4\Omega}{(2\pi)^3}\int_{q,p=0}^{\Lambda}\frac{1}{4q^2-\Omega_+^2}\left\{\frac{2G^-(r)}{1+r} + \frac{4pq+4q^2+4p^2-\Omega^2}{(4p^2+\Omega_+^2)}G^+(r) - \frac{2G^+(r)}{r}\frac{12q^2-\Omega^2}{4q^2+\Omega_+^2}\right\}, \tag{66}$$

$$G = \frac{2(1+r^2)}{3r}\log\frac{(1+r)^2}{(1-r)^2} - \frac{8}{3},$$

$$G^{\pm} = \frac{(1\mp r)^4}{6r^2}\log\frac{(1+r)^2}{(1-r)^2} \pm 4 - \frac{2(1\pm r)^2}{3r},$$

with $r = q/p$. The integrals give

$$\sigma_1(\Omega) = \frac{e^4\Omega}{9\pi^2}\left[-\log\frac{4\Lambda^2}{\Omega^2} - 5 + \frac{i}{8\pi}\log^2\frac{4\Lambda^2}{\Omega^2}\right]. \tag{67}$$

One observes that the subleading terms cannot be given correctly by the Weyl approximation as expected. We can use the renormalized velocity from Eq. (4) to make the real part finite.

C. Renormalization of the perturbative expansion for conductivity

We have calculated the renormalization of the Fermi velocity Eq. (4) and the ac conductivity of the clean Weyl semimetal within the leading order in Coulomb interaction. It is very tempting to try to use renormalization to improve the results of the bare perturbation theory presented to the leading order above by renormalizing the parameters of the theory. The expression for the ac conductivity both in the leading order and for the interaction correction contains dependence on the UV cutoff a or Λ and it is interesting to ask whether physically measurable quantities can be rewritten via "renormalized" parameters only or the microscopic details represented by the cutoff dependence are indeed unavoidable for certain measurable quantities like the ac conductivity.

The possibility of renormalizability is expected for the 3D Weyl model on the following two grounds.

(1) It has been claimed recently and shown to a very high order explicitly that the 2D version (graphene) is renormalizable.[27] This is surprising due to the breaking of the relativistic invariance (that ensures the renormalizability for a 2D model with a 3D electromagnetic coupling). The ac conductivity expression in 2D can be written via the renormalized Fermi velocity Eq. (4) replacing the bare one in Eq. (67). The key point here is that the leading order conductivity is independent of both the velocity and the UV cutoff.

(2) The relativistic version QED is renormalizable. Breaking of the relativistic invariance by taking just the static part of the interaction might not spoil this like in 2D.

We perform the renormalization of parameters up to the leading order. Replacing the bare Fermi velocity with the renormalized one from Eq. (4) in the real part of the conductivity from Eq. (8), the correction becomes finite and proportional to frequency:

$$\sigma' = \frac{e^2\Omega}{3\pi v_r}\left(1+\frac{\alpha}{3\pi}\log\frac{4v_r^2\Lambda^2}{\overline{\Omega}^2}\right) + \frac{e^2\alpha\Omega}{9\pi^2 v_r}\left(-\log\frac{4v_r^2\Lambda^2}{\Omega^2} - 5\right) = \frac{e^2\Omega}{3\pi v_r}\left[1+\frac{\alpha}{3\pi}\left(\log\frac{\Omega^2}{\overline{\Omega}^2}+C\right)+O(\alpha^2)\right], \tag{68}$$

where $\alpha = \frac{e^2}{v_r\hbar}$ leading to the result (in physical units) given in Eq. (8). As in 2D the constant C is positive and of order 1. Note that the coefficient e^2 in the definition of the current is not directly related by relativistic invariance to the Coulomb interaction in the present model, and thus is not renormalized. In the order considered there is no need to renormalize the static Coulomb coupling. The imaginary part Eq. (9) remains however "divergent," namely logarithmically dependent on microscopic details even after renormalization. This of course is not surprising due to the discussion of the imaginary part in the noninteraction theory in Sec. IV D. Even in the free case the imaginary part is nonuniversal, namely depends on microscopic details. The situation remains the same in the interacting theory.

VI. DISCUSSION, EXPERIMENTAL CONSEQUENCES

Before discussing the applicability of the results to materials proposed as realizations of the Weyl semimetal, let us summarize the electromagnetic properties of the clean 3D semimetals at zero temperature that can be extracted from the ac conductivity [Eqs. (6)–(9)]. The extension of our formulas to finite temperature was trivial via the Matsubara substitution $\Omega \to \Omega - i\pi k_B T/\hbar$; the dc conductivity of noninteracting Weyl plasma at finite temperature is given in Eq. (50).

The properties of the clean semimetal are expected to be dissimilar from those of a band insulator and a metal. In particular, the dielectric and optical properties differ markedly from both of them. The complex conductivity of the neutral Weyl plasma at zero temperature is very different from semiconductors and from metals. Let us contrast it with the Lorentz model of a band insulator and the Drude model for metals with electron density n and relaxation time τ. The ac conductivity of the Lorentz model of a band insulator (semiconductor), represented in Fig. 3 by the red line, is

$$\sigma_{\text{ins}}(\Omega) = \frac{\omega_p^2\tau}{4\pi}\frac{\Omega}{\Omega + i\tau\left(\omega_0^2-\Omega^2\right)}, \tag{69}$$

where the central frequency of the band was taken to be rather small $\omega_0 = 3\times 10^{14}$ Hz, the relaxation time

$\tau = 2 \times 10^{-14}$ s and the plasma frequency $\omega_p = 10^{14}$ Hz. The Drude conductivity of a metal, represented by the blue line, is obtained from this formula by taking $\omega_0 = 0$ and the values of $\tau = 2 \times 10^{-14}$ s and $\omega_p = 2 \times 10^{14}$ Hz. These are compared with the real part and the imaginary part, Figs. 3(a) and 3(b), respectively, of the Weyl semimetal, represented by the magenta line. The number of Weyl points is $N_W = 8$, the UV cutoff $\Lambda = \pi/a$, $a = 3$ A, $v = 10^6$ m/s, and the intrinsic dielectric constant $\epsilon = 3$ (due degrees of freedom not included in the model). At low frequencies the absorptive part is linear, so that at dc the Weyl semimetal is insulating. However it becomes comparable with that of (a poor) metal at THz frequencies. The imaginary part is linear as in a metal but with the opposite sign (capacitive like in insulator rather than inductive).

The complex dielectric constant of the 3D semimetal is $\varepsilon = 1 + 4\pi i\sigma/\Omega = \varepsilon' + i\varepsilon''$,

$$\begin{aligned} \varepsilon'(\Omega) &= 1 + \frac{N_W e^2}{3\pi v\hbar} \log \frac{\Lambda v}{\Omega}\left[1 + \frac{\alpha}{3\pi} \log \frac{\Lambda v}{\Omega}\right], \\ \varepsilon''(\Omega) &= \frac{N_W e^2}{6v\hbar}\left[1 + \alpha\left(\frac{2}{3\pi} \log \frac{\Omega}{\overline{\Omega}} + C\right)\right], \end{aligned} \tag{70}$$

where $\alpha = e^2/\epsilon v\hbar$ with the renormalized (measured) value of the Fermi velocity v. The normalization frequency is $\overline{\Omega}$ and $C = -\frac{5}{3\pi} \approx -0.53$.

The real part of the dielectric constant $\varepsilon' > 1$ is like that of an ordinary *dielectric* material with a very weak frequency dependence, see Fig. 4(a), despite the nonzero ac conductivity which is linear in frequency. Albeit note the logarithmic divergence for small frequencies: For example at $\Omega =$ 100 MHz, $\varepsilon' = 16$, see Fig. 4(a). The imaginary part of the dielectric constant depends also only weakly on frequency and is universal in that it is of order $0.2N_W$ for Fermi velocity $v \sim 10^6$ m/s and intrinsic dielectric constant $\epsilon = 3$.

Note also that unlike the imaginary part of the dielectric constant that is universal (insensitive to the microscopic details), the real part is dependent on the microscopic model and is therefore nonuniversal. This is seen already in the noninteracting model.

Let us compare the electric and optical properties of the pure 3D Weyl semimetal at neutrality point with the corresponding ones in 2D. In the pure 2D Weyl semimetal at the neutrality point (suspended undoped graphene is considered to be a good realization of this model[8]) the real part of the conductivity is finite and frequency independent in infinite samples and with no contact work function,[24] and there is no imaginary part in the ac conductivity, at least to leading order in interactions. The transport therefore is purely pseudodissipative. As noted before, the situation changes rather dramatically in 3D. We expect that problems of separation between the interband transitions (between the valence and the conduction bands or electron-hole pairs effects) considered in the present study and the intraband transitions (including the Klein scattering) due to potential barriers and mesoscopic effects are less pronounced in 3D compared to 2D. Let us now discuss the limitations of the model and point out some immediate extensions.

A clean system was assumed, while disorder is expected to be present. The effects of disorder, neglecting the interactions, were studied in Ref. 14. There might be an interplay between the disorder and interaction effects, but the basic physics is expected to be unaltered unless interaction or disorder are strong. One also can hope that, like in graphene, the importance of disorder might be reduced compared to expectations based on physics of ordinary "nonrelativistic" quasiparticles. The use of an approximation like the tight-binding model of Sec. II or even a continuum low energy Weyl model is justified as long as the frequencies considered are much lower than the bandwidth. As we argued in Sec. V, the tight-binding model is rather universal, but the use of the effective massless Weyl theory on the condensed matter scale has to be dealt with care.

It is well known in field theory[25] and in graphene that massless fermions cause the absence of a perfect scale separation between high energies (on atomic scale γ) and low energies (effective Weyl theory on the condensed matter scale $\ll \gamma$). It was demonstrated in the context of graphene[20] that some aspects of the linear response physics, including the Coulomb interactions corrections,[19] are *not* dominated by the Weyl points of the Brillouin zone at which the effective low energy model is valid. For example, large contributions (infinite, when the size of the Brillouin zone is being considered infinite) to the conductivity from the vicinity of the Weyl points are canceled by contributions from the region between them. Another famous consequence of this scale nonseparation is the "species doubling" of lattice fermions,[25] which in the context of graphene means that there necessarily appears a pair of Weyl points of opposite chirality. The UV regularization of the effective theory *does matter* and, if one were to use such a model, the only regularization known to date to be consistent with the tight binding is the space dimensional regularization developed in Ref. 17.

There are a number of quite straightforward extensions of the leading order interaction calculation of the ac conductivity performed in the present work. Converting it into the RPA-like approximation is simple, but in addition taking into account the finite momentum transfer is more involved than the analogous calculations in graphene.[18] This would allow us to study the plasmons' effects and even the strong coupling phenomena like the exciton condensation.[28] Beyond the linear response, phenomena like the nonlinear I-V curves due to the particle-hole (Schwinger) pair creation and relaxation due to their recombination studied in the context of graphene[29] also can be extended to 3D in a straightforward fashion.

ACKNOWLEDGMENTS

We are indebted to T. Maniv, H. C. Kao, and W. B. Jian for valuable discussions.

APPENDIX A: THE UNIVERSAL TIGHT-BINDING MODEL

1. Diagonalization of the noninteracting tight-binding model and expression for the current

The noninteracting model is diagonalized in 3D with the following coefficients of the Bogoliubov transformation

Eq. (18):

$$u_{\mathbf{k}} = \frac{1}{\sqrt{2\varepsilon_k(\varepsilon_k+\widehat{k}_z)}}\begin{pmatrix} -\widehat{k}_x + i\widehat{k}_y \\ \varepsilon_k + \widehat{k}_z \end{pmatrix},$$
$$v_{\mathbf{k}} = \frac{1}{\sqrt{2\varepsilon_k(\varepsilon_k+\widehat{k}_z)}}\begin{pmatrix} \varepsilon_k + \widehat{k}_z \\ \widehat{k}_x + i\widehat{k}_y \end{pmatrix}, \tag{A1}$$

where $\widehat{k} \equiv \sin k$ and $\varepsilon_k^2 = \widehat{k}_x^2 + \widehat{k}_y^2 + \widehat{k}_z^2$. Using matrix elements

$$u_k^+\sigma_3 v_k = -\frac{\widehat{k}_x + i\widehat{k}_y}{\varepsilon_k}, \quad v_k^+\sigma_3 v_k = -u_k^+\sigma_3 u_k = \frac{\widehat{k}_z}{\varepsilon_k}, \tag{A2}$$

one obtains the coefficient of the electric current as

$$\chi_{\mathbf{k}} = \frac{(\widehat{k}_y - i\widehat{k}_x)\cos k_z}{\varepsilon_k}, \quad \iota_{\mathbf{k}} = \frac{\widehat{k}_z \cos k_z}{2\varepsilon_k}. \tag{A3}$$

2. Normal ordering of the interaction

The normal ordering is quite straightforward:

$$V^{ij} = \sum_{klk'l'} v_{klk'l'} O^{ij}, \tag{A4}$$

where the part V^{ij} contains i creation operators a^+ or b^+ and j annihilation operators a or b. The quartic terms are

$$O^{40} = -(v_l^* \cdot u_k)(v_{l'}^* \cdot u_{k'}) a_l^+ a_{l'}^+ b_{-k}^+ b_{-k'}^+ = (O^{04})^+, \tag{A5}$$

$$\begin{aligned} O^{31} = (O^{13})^+ &= (v_l^* \cdot u_k)[(v_{l'}^* \cdot v_{k'}) a_l^+ b_{-k}^+ a_{l'}^+ a_{k'} \\ &- (u_{l'}^* \cdot u_{k'}) a_l^+ b_{-k}^+ b_{-k'}^+ b_{-l'}] + (v_{l'}^* \cdot u_{k'}) \\ &\times [(v_l^* \cdot v_k) a_l^+ a_{l'}^+ b_{-k'}^+ a_k - (u_l^* \cdot u_k)] a_{l'}^+ b_{-k}^+ b_{-l} b_{-k'}^+, \end{aligned} \tag{A6}$$

$$\begin{aligned} O^{22} = &-(v_{l'}^* \cdot v_{k'})(v_l^* \cdot v_k) a_l^+ a_{l'}^+ a_k a_{k'} + (u_l^* \cdot u_k)(v_{l'}^* \cdot v_{k'}) \\ &\times a_{l'}^+ b_{-k}^+ a_{k'} b_{-l} + (u_{l'}^* \cdot u_{k'})(v_l^* \cdot v_k) a_l^+ b_{-k'}^+ a_k b_{-l'} \\ &- (u_l^* \cdot u_k)(u_{l'}^* \cdot u_{k'}) b_{-k}^+ b_{-k'}^+ b_{-l} b_{l'} - (v_l^* \cdot u_k)(u_{l'}^* \cdot v_{k'}) \\ &\times a_l^+ b_{-k}^+ a_{k'} b_{-l'} - (u_l^* \cdot v_k)(v_{l'}^* \cdot u_{k'}) a_l^+ b_{-k'}^+ a_k b_{-l}. \end{aligned} \tag{A7}$$

In principle there are three possible quadratic terms where

$$\begin{aligned} O^{20} &= (O^{02})^+ = \delta_{k-l'}(v_l^* \cdot v_k)(v_{l'}^* \cdot u_{k'}) a_l^+ b_{-k'}^+ \\ &- \delta_{l-k'}(u_l^* \cdot u_k)(v_{l'}^* \cdot u_{k'}) a_{l'}^+ b_{-k}^+. \\ O^{11} &= \delta_{k-l'}(v_{l'}^* \cdot v_{k'})(v_l^* \cdot v_k) a_l^+ a_{k'} + \delta_{l-k'}(u_l^* \cdot u_k)(u_{l'}^* \cdot u_{k'}) b_{-k}^+ \\ &\times b_{-l'} - (u_l^* \cdot v_k)(v_{l'}^* \cdot u_{k'})(\delta_{k-l'} b_{-k'}^+ b_{-l} + \delta_{l-k'} a_{l'}^+ a_k). \end{aligned} \tag{A8}$$

Relations between the scalar products for unequal momenta that appear here

$$(u_k^* \cdot u_l) = (v_k^* \cdot v_l)^*, \quad (v_k^* \cdot u_l) = -(u_k^* \cdot v_l)^* = -(v_l^* \cdot u_k) \tag{A9}$$

are useful in summation over momenta incorporating Eq. (24), in particular for two equal momenta

$$v_{klk'k} = \frac{1}{\mathcal{V}} v_{l-k}\delta_{l-k'}, \quad v_{kk'k'l'} = \frac{1}{\mathcal{V}} v_{k'-k}\delta_{l'-k}. \tag{A10}$$

Most importantly, summing over momenta, the pair creation term vanishes:

$$\begin{aligned} V^{20} &= \sum_{kl} v_{l-k}(-(u_l^* \cdot v_k)(v_k^* \cdot v_l) b_{-l}^+ a_l^+ \\ &+ (u_l^* \cdot v_k)(u_k^* \cdot u_l) b_{-k}^+ a_k^+) \\ &= \sum_{kl} v_{l-k}(u_l^* \cdot v_k)((u_l^* \cdot u_k) - (v_k^* \cdot v_l)) b_{-l}^+ a_l^+ = 0. \end{aligned} \tag{A11}$$

This leads to numerous simplifications.

APPENDIX B: ANGLE INTEGRALS APPEARING IN CALCULATIONS OF SELF-ENERGY AND CONDUCTIVITY

1. Self-energy

The integral over $\phi_{\mathbf{q}}$ in Eq. (33) for the self-energy is, using

$$\int_{\Delta=0}^{2\pi} \frac{c + d\cos\Delta}{a + b\cos\Delta} = \frac{2\pi}{b}[(bc - ad)/\sqrt{a^2 - b^2} + d], \tag{B1}$$

is

$$\begin{aligned} &\frac{1}{2\pi}\int_{\phi_q=0}^{2\pi} \frac{\cos\theta_q\cos\theta_p + \sin\theta_q\sin\theta_p\cos(\phi_p - \phi_q)}{1 + r^2 - 2r[\cos\theta_p\cos\theta_q + \sin\theta_p\sin\theta_q\cos(\phi_p - \phi_q)]} \\ &= \frac{1}{2r}\left[\frac{1 + r^2}{\sqrt{(1 + r^2 - 2r\cos\theta_p\cos\theta_q)^2 - (2r\sin\theta_p\sin\theta_q)^2}} - 1\right]. \end{aligned} \tag{B2}$$

The integral over the azimuth angle for $\theta_p = 0$ (our choice for the quasiparticle direction) results in

$$\frac{1}{2\pi}\int_{\theta_q=0}^{\pi} \sin\theta_q\left(\frac{1 + r^2}{1 + r^2 - 2r\cos\theta_q} - 1\right) = \frac{1 + r^2}{2r^2}\log\frac{(1 + r)^2}{(1 - r)^2} - \frac{2}{r}, \tag{B3}$$

leading to Eq. (34).

2. Corrections to conductivity

First contribution to the ac conductivity, Eq. (61), involves the angle integral

$$I_1 = \int_{\phi_p\phi_q\theta_p\theta_q} \sin\theta_p \sin\theta_q \frac{\sin^2\theta_q[\cos\theta_q\cos\theta_p + \sin\theta_q\sin\theta_p\cos(\phi_p-\phi_q)]}{p^2+q^2-2pq[\cos\theta_p\cos\theta_q+\sin\theta_p\sin\theta_q\cos(\phi_p-\phi_q)]}. \tag{B4}$$

Integration over ϕ_p and $\Delta\phi = \phi_p - \phi_q$ using Eq. (B1) gives

$$I_1 = \frac{2\pi^2}{r}\int_{\theta_p\theta_q} \sin\theta_p \sin^3\theta_q \left[\frac{1+r^2}{\sqrt{(1+r^2-2r\cos\theta_p\cos\theta_q)^2-(2r\sin\theta_p\sin\theta_q)^2}} - 1\right] = \frac{2\pi^2}{r}G^+(r), \tag{B5}$$

where function G^+ is given in Eq. (66). The two other angle integrals are done in the same way.

*vortexbar@yahoo.com

[1] P. A. Wolff, J. Phys. Chem. Sol. **25**, 1057 (1964).

[2] P. Hosur, S. Ryu, and A. Vishwanath, Phys. Rev. B **81**, 045120 (2010); X. Wan, A. M. Turner, A. Vishwanath, and S. Y. Savrasov, *ibid.* **83**, 205101 (2011).

[3] T. Kariyado and M. Ogata, J. Phys. Soc. Jpn. **80**, 083704 (2011); **81**, 064701 (2012); P. Delplacel, J. Li, and D. Carpentier, Europhys. Lett. **97**, 67004 (2012).

[4] S. M. Young, S. Zaheer, J. C. Y. Teo, C. L. Kane, E. J. Mele, and A. M. Rappe, Phys. Rev. Lett. **108**, 140405 (2012); Z. Wang, Y. Sun, X. Q. Chen, C. Franchini, G. Xu, H. Weng, X. Dai, and Z. Fang, Phys. Rev. B **85**, 195320 (2012); A. Go, W. Witczak-Krempa, G. S. Jeon, K. Park, and Y. B. Kim, Phys. Rev. Lett. **109**, 066401 (2012); W. Witczak-Krempa and Y. B. Kim, Phys. Rev. B **85**, 045124 (2012).

[5] A. A. Burkov and L. Balents, Phys. Rev. Lett. **107**, 127205 (2011); A. A. Zyuzin, S. Wu, and A. A. Burkov, Phys. Rev. B **85**, 165110 (2012).

[6] G. Xu, H. Weng, Z. Wang, X. Dai, and Z. Fang, Phys. Rev. Lett. **107**, 186806 (2011); C. Fang, M. J. Gilbert, X. Dai, and B. A. Bernevig, *ibid.* **108**, 266802 (2012).

[7] M. I. Katsnelson, *Graphene: Carbon in Two Dimensions* (Cambridge University Press, Cambridge, 2012).

[8] X. Du, I. Skachko, A. Barker, and E. Y. Andrei, Nat. Nano. **3**, 491 (2008); K. I. Bolotin, K. J. Sikes, J. Hone, H. L. Stormer, and P. Kim, Phys. Rev. Lett. **101**, 096802 (2008); A. S. Mayorov *et al.*, Nano Lett. **12**, 4629 (2012).

[9] P. R. Wallace, Phys. Rev. **71**, 622 (1947).

[10] K. Wang, D. Graf, H. Lei, S. W. Tozer, and C. Petrovic, Phys. Rev. B **84**, 220401 (2011); K. Ueda, J. Fujioka, Y. Takahashi, T. Suzuki, S. Ishiwata, Y. Taguchi, and Y. Tokura, Phys. Rev. Lett. **109**, 136402 (2012); F. F. Tafti, J. J. Ishikawa, A. McCollam, S. Nakatsuji, and S. R. Julian, Phys. Rev. B **85**, 205104 (2012); J. J. Ishikawa, E. C. T. O'Farrell, and S. Nakatsuji, *ibid.* **85**, 245109 (2012); S. Boseggia, R. Springell, H. C. Walker, H. M. Ronnow, Ch. Ruegg, H. Okabe, M. Isobe, R. S. Perry, S. P. Collins, and D. F. McMorrow, Phys. Rev. Lett. **110**, 117207 (2013).

[11] B. M. Anderson, G. Juzeliunas, V. M. Galitski, and I. B. Spielman, Phys. Rev. Lett. **108**, 235301 (2012); J. H. Jiang, Phys. Rev. A **85**, 033640 (2012).

[12] P. Soltan-Panahi, J. Struck, P. Hauke, A. Bick, W. Plenkers, G. Meineke, C. Becker, P. Windpassinger, M. Lewenstein, and K. Sengstock, Nat. Phys. **7**, 434 (2011); Z. Lan, A. Celi, W. Lu, P. Ohberg, and M. Lewenstein, Phys. Rev. Lett. **107**, 253001 (2011); K. Sun, W. V. Liu, A. Hemmerich, and S. Das Sarma, Nat. Phys. **8**, 67 (2012).

[13] Y. Fuseya, M. Ogata, and H. Fukuyama, J. Phys. Soc. Jpn. **81**, 013704 (2012).

[14] G. B. Jo, J. Guzman, C. K. Thomas, P. Hosur, A. Vishwanath, and D. M. Stamper-Kurn, Phys. Rev. Lett. **108**, 045305 (2012).

[15] I. F. Herbut, V. Juricic, and O. Vafek, Phys. Rev. Lett. **100**, 046403 (2008).

[16] E. G. Mishchenko, Phys. Rev. Lett. **98**, 216801 (2007); D. E. Sheehy and J. Schmalian, *ibid.* **99**, 226803 (2007); E. G. Mishchenko, Europhys. Lett. **83**, 17005 (2008).

[17] V. Juričić, O. Vafek, and I. F. Herbut, Phys. Rev. B **82**, 235402 (2010).

[18] V. N. Kotov, B. Uchoa, and A. H. Castro Neto, Phys. Rev. B **78**, 035119 (2008); S. H. Abedinpour, G. Vignale, A. Principi, M. Polini, W. K. Tse, and A. H. MacDonald, *ibid.* **84**, 045429 (2011); I. Sodemann and M. M. Fogler, *ibid.* **86**, 115408 (2012).

[19] B. Rosenstein, M. Lewkowicz, and T. Maniv, Phys. Rev. Lett. **110**, 066602 (2013).

[20] H. C. Kao, M. Lewkowicz, and B. Rosenstein, Phys. Rev. B **82**, 035406 (2010).

[21] M. A. H. Vozmediano and F. Guinea, Nucl. Phys. T **146**, 014015 (2001); J. Gonzalez, F. Guinea, and M. A. H. Vozmediano, Phys. Rev. B **59**, R2474 (1999).

[22] M. Lewkowicz and B. Rosenstein, Phys. Rev. Lett. **102**, 106802 (2009).

[23] K. Ziegler, Phys. Rev. Lett. **97**, 266802 (2006); Phys. Rev. B **75**, 233407 (2007); S. Ryu, C. Mudry, A. Furusaki, and A. W. W. Ludwig, *ibid.* **75**, 205344 (2007).

[24] M. Lewkowicz, B. Rosenstein, and D. Nghiem, Phys. Rev. B **84**, 115419 (2011).

[25] J. Smit, *Introduction to Quantum Fields on a Lattice* (Cambridge University Press, New York, 2002).

[26] J. E. Drut and T. A. Lahde, Phys. Rev. Lett. **102**, 026802 (2009); Phys. Rev. B **79**, 165425 (2009); P. V. Buividovich, E. V. Luschevskaya, O. V. Pavlovsky, M. I. Polikarpov, and M. V. Ulybyshev, *ibid.* **86**, 045107 (2012); P. V. Buividovich and M. I. Polikarpov, *ibid.* **86**, 245117 (2012); M. V. Ulybyshev, P. V. Buividovich, M. I. Katsnelson, and M. I. Polikarpov, arXiv:1304.3660.

[27]F. de Juan, A. G. Grushin, and M. A. H. Vozmediano, Phys. Rev. B **82**, 125409 (2010); A. Politano, A. R. Marino, and G. Chiarello, *ibid.* **82**, 155404 (2010); **86**, 085420 (2012).

[28]M. A. H. Vozmediano and F. Guinea, Phys. Scripta **T146**, 014015 (2012); H. Wei, S.-P. Chao, and V. Aji, Phys. Rev. Lett. **109**, 196403 (2012).

[29]A. Barreiro, M. Lazzeri, J. Moser, F. Mauri, and A. Bachtold, Phys. Rev. Lett. **103**, 076601 (2009); N. Vandecasteele, A. Barreiro, M. Lazzeri, A. Bachtold, and F. Mauri, Phys. Rev. B **82**, 045416 (2010); M. I. Katsnelson and G. E. Volovik, JETP Lett. **95**, 411 (2012); M. I. Katsnelson, G. E. Volovik, and M. A. Zubkov, Ann. Phys. **331**, 160 (2013).